General Disclaimer

One or more of the Following Statements may affect this Document

- This document has been reproduced from the best copy furnished by the organizational source. It is being released in the interest of making available as much information as possible.

- This document may contain data, which exceeds the sheet parameters. It was furnished in this condition by the organizational source and is the best copy available.

- This document may contain tone-on-tone or color graphs, charts and/or pictures, which have been reproduced in black and white.

- This document is paginated as submitted by the original source.

- Portions of this document are not fully legible due to the historical nature of some of the material. However, it is the best reproduction available from the original submission.

NASA Technical Memorandum 83402

Cavitation Erosion of Copper, Brass, Aluminum, and Titanium Alloys in Mineral Oil

B. C. S. Rao and D. H. Buckley
Lewis Research Center
Cleveland, Ohio

Prepared for the
Sixth International Conference on Erosion
by Liquid and Solid Impact
sponsored by the Cavendish Laboratory
Cambridge, England, September 4–8, 1983

NASA

CAVITATION EROSION OF COPPER, BRASS, ALUMINUM, AND TITANIUM ALLOYS IN MINERAL OIL

B. C. S. Rao* and D. H. Buckley

National Aeronautics and Space Administration
Lewis Research Center
Cleveland, Ohio 44135

ABSTRACT

The variations of the mean depth of penetration MDP, the mean depth rate of penetration MDRP, the pit diameter 2a and depth h due to cavitation attack on Al 6061-T6, Cu, brass of composition Cu-35.5Zn-3Pb and Ti-5Al-2.5Sn are presented. The experiments are conducted in a mineral oil of viscosity 110 CS using a magnetostrictive oscillator of 20 kHz frequency. Based on MDRP on the materials, it is found that Ti-5Al-2.5Sn exhibits cavitation erosion resistance which is two orders of magnitude higher than the other three materials. The values of h/a are the largest for copper and decreased with brass, titanium and aluminum. Scanning electron microscope studies show that extensive slip and cross-slip occurred on the surface prior to pitting and erosion. Twinning is also observed on copper and brass.

E-1614

INTRODUCTION

The occurrence of cavitation erosion in bearings has been reported (1) in increasing frequency in recent years. This phenomenon is predominantly observed in diesel engine bearings and on rare occassions in gasoline engines when operated under sustained overspeed or with incorrect ignition timing. Many examples of the occurrence of cavitation erosion in bearings (e.g. 2), in gears (3) and other equipment using oils (4) are reported in the literature.

A large amount of data on cavitation erosion of different materials in water exists in the literature at this time, although its precise mechanism is still not well understood. A few investigations on cavitation erosion in oils and liquids other than water have also been reported recently. The authors are currently carrying out a study of the cavitation erosion of different bearing metals and alloys in mineral oils. This paper presents the variations of mean depth of penetration, mean depth rate of penetration, the pit diameter and depth due to cavitation attack on copper, yellow brass, aluminum, and a titanium alloy. The eroded surfaces of these materials have been scanned through an electron microscope at different stages and the results of these observations are included.

*NRC-NASA Research Associate.

EXPERIMENTAL EQUIPMENT AND TEST CONDITIONS

The experiments were carried out in an ultrasonic magnetostrictive oscillator operating at 20 kHz frequency and a peak-to-peak amplitude of 50μm. The test specimens for the experiments are prepared from rods of 12.7 mm diameter of aluminum 6061-T6, copper C 11 000 (electrolytic), free cutting brass and titanium Ti-5Al-2.5Sn. The mechanical properties of these materials are presented in Table I. The cavitation erosion experiments are conducted in a mineral oil whose physical properties are given in Table II. The test surface of the specimens has been finished to a roughness of less than 1 μm.

The test specimen is subjected to cavitation action in mineral oil and weight loss measurements are taken at intervals of 1 to 5 minutes in the case of aluminum, copper and brass and at intervals of 30 to 120 minutes on the titanium alloy. For comparison purposes, cavitation erosion experiments are also conducted on aluminum in ordinary tap water.

EXPERIMENTAL RESULTS

Mean depth of penetration MDP. - Figure 1 presents the mean depth of penetration on the four different materials with test time. The mean depth of penetration MDP at any test time is computed as:

$$MDP = \frac{\Delta W_c}{\rho_m A_m} \qquad (1)$$

where ΔW_c = cumulative weight loss
ρ_m = density of test material
and A_m = surface area of test specimen.

Among the materials tested, copper exhibited least resistance to erosion although the erosion on aluminum, copper and brass is of comparable magnitude. The titanium alloy exhibited the maximum resistance with a MDP of 15 μm in 30 hours.

Figures 2(a), (b), (c) and (d) present the mean depth rate of penetration (MDRP) of copper, brass, aluminum and titanium alloy, respectively. It may be noted again that the MDRP of copper, brass and aluminum is about two orders of magnitude larger than that of the titanium alloy.

Cavitation pits. - The nature of cavitation pits are generally assumed to be spherical segments as shown in Figure 3. If $2a$ is the chord diameter and h is the depth of pit, the radius γ_2 of the sphere may be expressed as:

$$\gamma_2 = \frac{a^2 + h^2}{2h} \qquad (2)$$

Eq. (2) may be rewritten as:

$$\log (h/a) + \frac{1}{2} \log (2\gamma_2/h - 1) = 0 \qquad (3)$$

Surface profiles of the specimens subjected to cavitation action were taken at different time intervals using a profilometer. Using the measured values of a and h, the radii γ_2 of the spheres are computed according to Eq. (2). A plot of the logarithm of (h/a) with the logarithm of $(2\gamma_2/h - 1)$ for the four different materials is presented in Figure 4. Results of similar measurements on Al 6061-T6 in water carried out in an earlier study (5) are also included in the figure. It may be seen that the values of h/a are the largest on copper, and those of brass, titanium alloy and aluminum follow in the decreasing order. In other words, for the same depth, the width of pits is larger on brass, titanium and aluminum than those on copper. The maximum depth of pits measured on titanium was about 15 μm at the end of 30 hours while on the other three materials the depth of pits was about 250 μm. Also, compared to the cavitation pits in water, the cavitation pits in mineral oil were smaller in size and larger in number.

Electron microscope investigations. - The surfaces of the specimens subjected to cavitation attack were examined under both optical and scanning electron microscopes. Some of the pictures taken on the surface of the brass specimen are included here. The approximate composition of brass studied is as follows:

Copper	61.5 percent
Zinc	35.5 percent
Lead	3 percent

This material was examined at 5 minute intervals of cavitation attack. The erosion at the end of first 5 minutes commenced in six different areas of size approximately 0.75x0.50 mm around the specimen and spread over the surface with increase of test time. One such eroded area observed at the end of first 5 minutes of cavitation attack is presented in Figure 5. The surface area attacked by cavitation erosion at the end of 40 minutes is shown in Figure 6. The grain boundary attack in the initial stages before erosion commenced may also be seen in Figure 5.

The observations using scanning electron microscope show that cavitation attack is highly localized with respect to individual grains. The deformation and pitting preceding erosion are related to the crystal structure of the material. The indentations observed on the surface suggest a thin microjet cavitation attack rather than the shockwave attack. Each crystal responded to the cavitation attack depending upon the state of stress already existing in it. The initial attack appears to be confined largely to grain boundaries and imperfections in the crystal. Extensive slip occured across the crystals during the early stages of deformation. Twinning is observed on copper and brass but not on aluminum and titanium alloy. The characteristic noise of twinning could be clearly heard during experimentation with copper and brass.

Figure 7(a) presents evidence of slip on a single grain of brass. Figure 7(b) presents a region showing extensive slip and cross-slip across the grains. The brass used in the experiments contains the α-, β and lead phases. The dark spots and lines seen in Figure 7(b) are the lead phase. The grain in the middle where slip lines are absent is the β-phase. Cavitation indentations at the grain boundaries could also be seen in Figure 7(b).

Figures 8(a) and (b) show areas where pit formation is developing. Extensive slip and cross-slip may again be seen in these figures. The pit formation is seen to be intercrystalline.

DISCUSSION

Collapse times and pressures. - In the present experiments using a magnetostrictive oscillator, the growth and collapse phases of the cavitation bubbles are restricted to one-quarter cycle of the oscillator, viz. 12.5 μ sec. Experimental observations (6) of the collapse phase show that it occurs in a period of about 5 μ sec in water. The mineral oil used in the present experiments is about 100 times viscous compared to water. The viscous effects considerably alter the pressure at the bubble wall and thus act to reduce the effective pressure differential so as to reduce the rates of both the bubble growth and collapse. The pressure $P(R)$ at the bubble wall during collapse may be expressed as:

$$P(R) = P_1(R) - \frac{2\sigma}{R} + \frac{4\mu U}{R} \qquad (4)$$

where

$P_i(R)$ = total vapor and gas pressure in the bubble
R = bubble radius
σ = surface tension
μ = viscosity of liquid
U = bubble wall collapse velocity, $\frac{dR}{dt}$
t = time

Observation of the eroded surfaces suggest that the cavitation bubbles grow to smaller sizes in mineral oil than in water. Hence, the size of microjets striking the surfaces in mineral oil are also smaller than those in water. The size of microjets generally observed in water is 1 to 10 μm. The size of indentations observed in the present studies in the initial stages range from less than 1 μm to a few micrometers.

The observation of extensive slip explains the reason for the existence of incubation periods during cavitation erosion of materials. Also, previous attempts (7, 8, 9) to relate the energy absorbed by the material considering the pit volume and the energy of collapse of cavitation bubbles showed a large gap between the two quantities. Recently, Hammitt and De (9) showed that the ratio of erosive power to acoustic power is approximately 10^{-6} for erosion data on 1100-0 aluminum. The authors expect this ratio to be of the order of 10^{-8} for cobalt, titanium and other metals and alloys of close-packed hexagonal (c.p.h.) crystal structure. It may be stated that a large proportion of the collapse energy is spent in macro- and micro-deformation of the individual crystals of a material in addition to that spent in pit formation.

The present observations also explain the excellent erosion resistance of materials such as cobalt, titanium and their alloys. It is very well known that metals such as aluminum and copper with face-centered-cubic (f.c.c.) crystal structures have four sets of {111} slip planes and three sets of [110] slip directions. In metals such as cobalt and titanium with a close-packed hexagonal (c.p.h.) crystal structure, slip is restricted to only one set of {001} planes in the three sets of [100] directions. The present studies indicate that the deformation and pitting of materials during cavitation attack is related to the crystal structure and the specific crystallographic planes of the metals and alloys.

CONCLUSIONS

1. Based on the mean depth rate of penetration, MDRP, it is found that the cavitation erosion resistance of Ti-5Al-2.5Sn alloy is two orders of magnitude higher than that for Cu, Cu-35.5Zn-3Pb brass and Al 6061-T6.

2. The ratio h/a of the pit depth h to the pit radius a is found to have largest values for copper and those for brass, titanium alloy and aluminum follow in the decreasing order.

3. Scanning electron microscope studies show that cavitation attack is highly localized with respect to the individual crystals of the materials. The initial attack is confined to grain boundaries and crystal imperfections.

4. Extensive slip and cross-slip are observed on all the four materials before pit formation. Twinning is also observed on copper and brass. The characteristic noise of twinning was audible during experimentation with these two materials. The material deformation and pitting are related to the crystallographic planes of the different metals and alloys.

REFERENCES

1. Garner D. R., James R. D. and Warriner J. F. 1980. J. Eng. Power 102, 847.
2. Dowson D. and Taylor C. M. 1979. Annu. Rev. Fluid Mech. 11, 35.
3. Hunt J. B., Ryde-Weller A. J., and Ashmead A. H. 1981, Wear 71, 65.
4. Heathcock C. J. and Protheroe B. E. 1982, Wear 81, 311.
5. Rao B. C. S. and Buckley D. H. 1982, NASA-TM-83345, also 1983 Cavitation and Polyphase Flow Forum, ASME.
6. Vyas B. and Preece C. M. 1976, J. of Appl. Phy. 47, 5133.
7. Thiruvengadam A. 1963. J. Basic Eng. 85, 365.
8. Rao B. C. S. 1969, Ph.D Thesis, Indian Inst. of Science, Bangalore.
9. Hammitt F. G. and De M. K. 1979. Wear, 55, 221.

TABLE I. - MECHANICAL PROPERTIES OF MATERIALS[a]

Material	Density, kg/m^3	Yield strength, MN/m^2	Tensile strength, MN/m^2	Elastic modulus, MN/m^2	Ultimate resilience, MN/m^2	Elongation, percent	Hardness
Aluminum 6061-T6	2700	276	310	$71x10^3$	0.54	12	95[b]
Copper	8100	303	330	$117x10^3$	0.54	16	38[b]
Brass (Cu-35.5-Zn-3Pb)	8500	276	379	$96.5x10^3$	0.74	32	47[c]
Ti-5Al-2.5Sn	4460	793	862	$110x10^3$	3.38	14	-

[a]From Metals Handbook, Vol. I, American Society of Metals, Metals Park, Ohio, 1967.
[b]Bhn.
[c]Rockwell B.

TABLE II. - PHYSICAL PROPERTIES OF MINERAL OIL

Property	Mineral Oil
Density, kg/m^3	869
Kinematic viscosity, CS at 20° C	110
Surface tension dynes/cm at 20° C	33.2
Bulk modulus, MPa	$1.7x10^3$
Flash point, °C	213
Pour point, °C	- 9.4

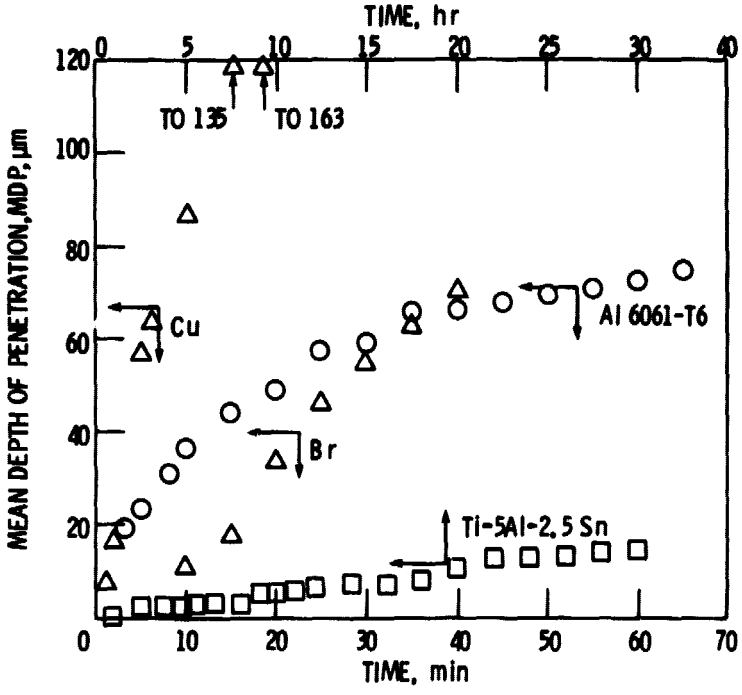

Figure 1. - Variation of mean depth of penetration MDP with test time.

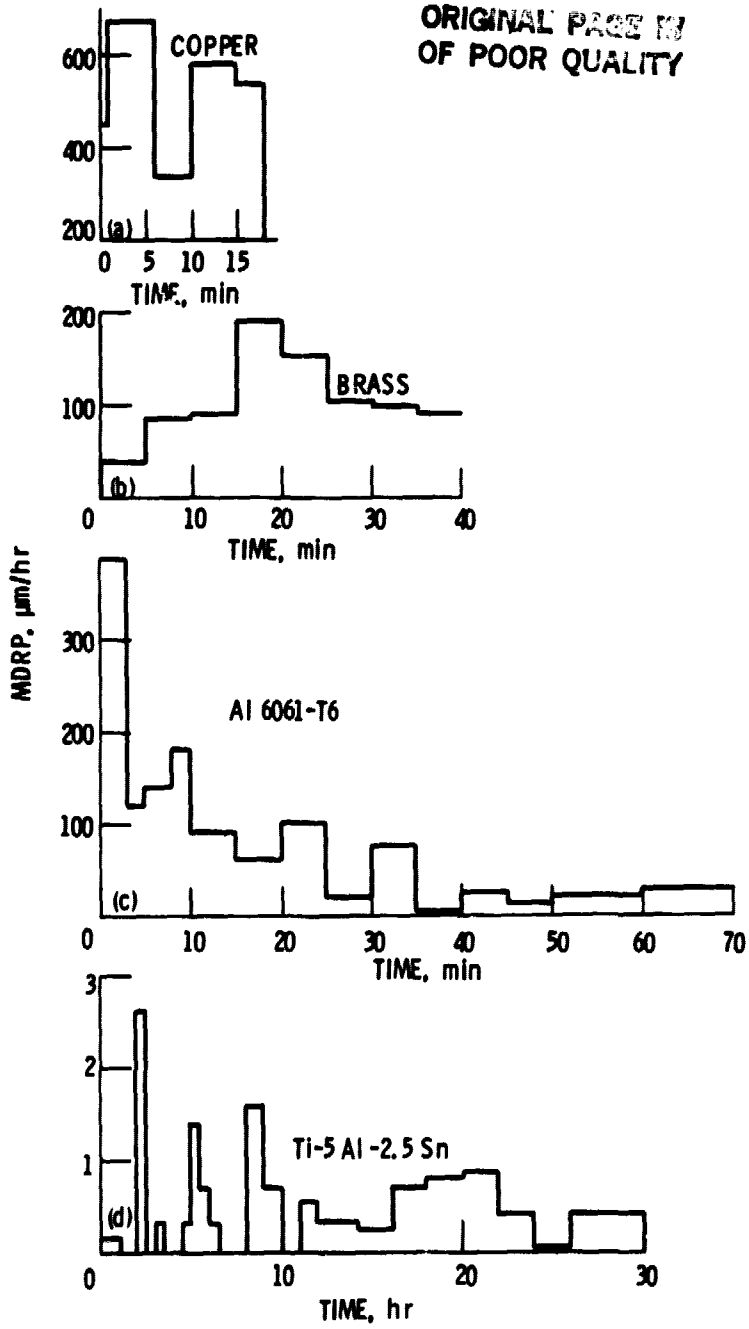

Figure 2. - Variation of mean depth rate of penetration MDRP with test time.

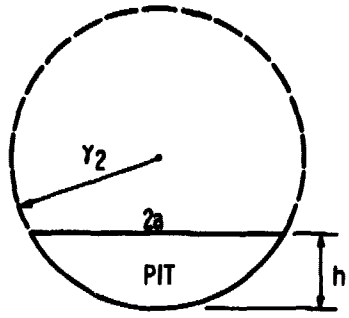

Figure 3. - Theoretical cavitation pit.

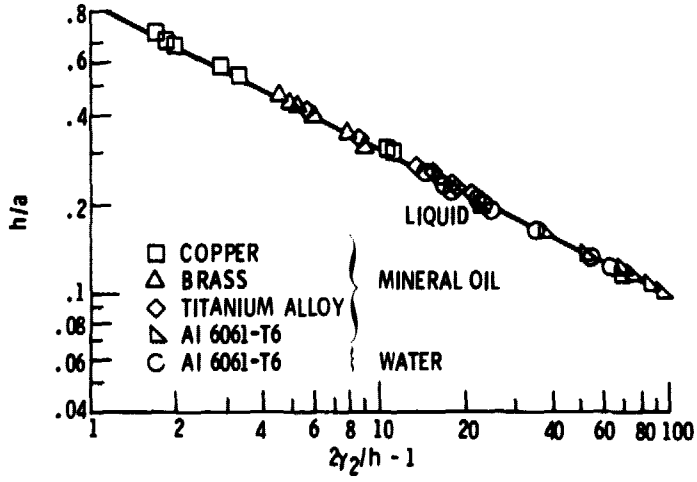

Figure 4. - Variation of h/a with $2r_2/h - 1$ of the cavitation pits.

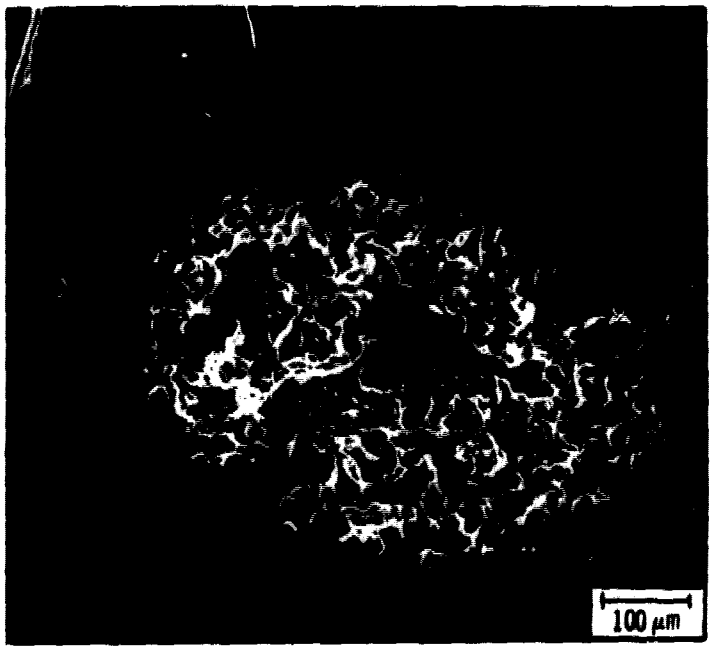

Figure 5. - Eroded area observed at the end of first 5 minutes on brass.

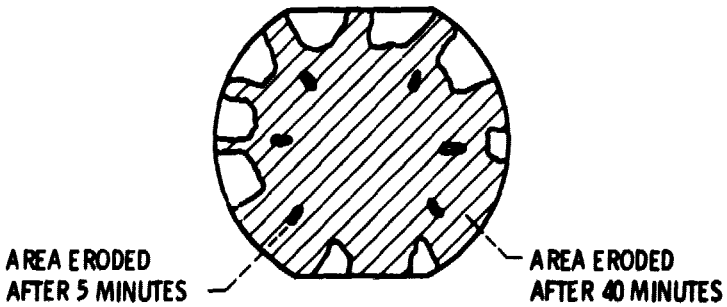

Figure 6. - Surface area eroded at the end of 40 minutes on brass.

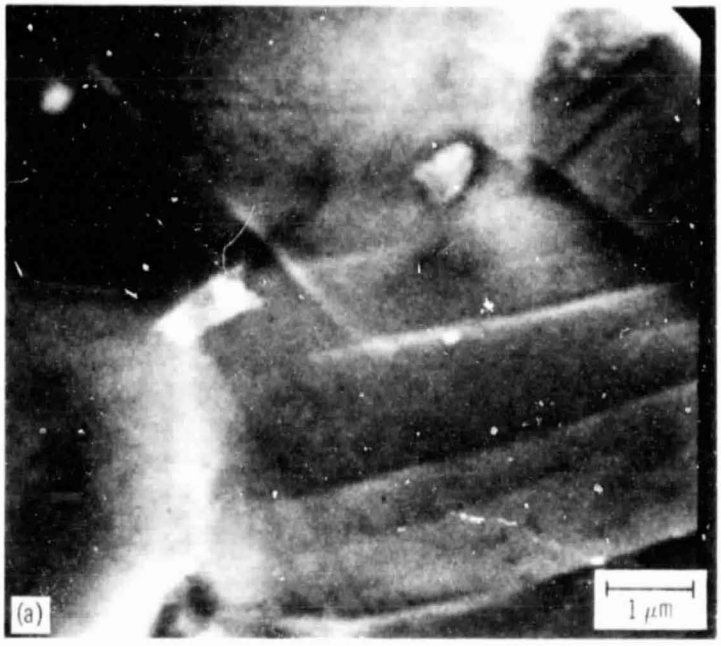

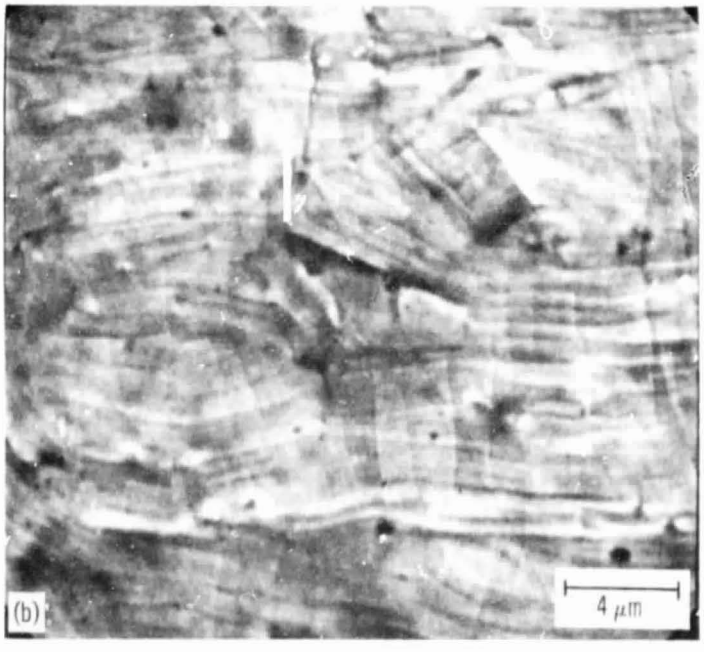

Figure 7. - Slip lines across crystals: (a) an individual crystal; (b) a group of crystals.

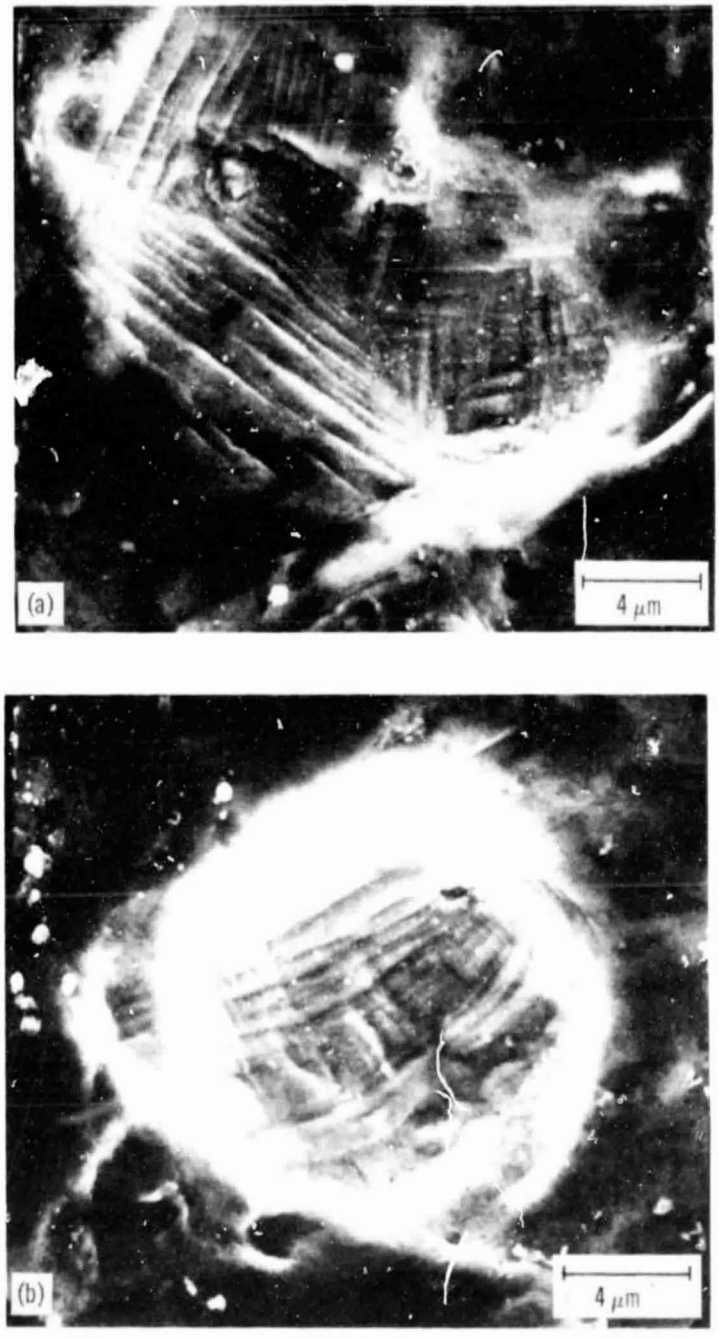

Figure 8. - Development of individual cavitation pits.